Hindawi
International Journal of Antennas and Propagation
Volume 2019, Article ID 3059480, 8 pages
https://doi.org/10.1155/2019/3059480

Research Article

Circularly Polarized Wearable Antenna Based on NinjaFlex-Embedded Conductive Fabric

Jianxiong Li[1,2] **Yuchen Jiang**[1,2] **and Xiaoming Zhao**[3]

[1]*School of Electronics and Information Engineering, Tianjin Polytechnic University, Tianjin 300387, China*
[2]*Tianjin Key Laboratory of Optoeletronic Detection Technology and Systems, Tianjin 300387, China*
[3]*School of Textile Science and Engineering, Tianjin Polytechnic University, Tianjin 300387, China*

Correspondence should be addressed to Jianxiong Li; lijianxiong@tjpu.edu.cn

Received 19 February 2019; Revised 5 June 2019; Accepted 4 July 2019; Published 8 September 2019

Academic Editor: Luca Catarinucci

A circularly polarized (CP) wearable antenna based on the FDM (fused deposition modeling) technology is proposed. Conductive fabric is used to realize conductive parts of the patch antenna on the NinjaFlex substrate. The antenna is encapsulated with additional layers of NinjaFlex. Modified patch ensures the CP character at 2.45 GHz. Bending and washing tests are conducted to check the performance stability, and good agreement between simulated and measured results is observed. The experimental results illustrate that the antenna holds 11% 10 dB S_{11} bandwidth and around 70 MHz 3 dB axial ratio bandwidth. In addition, surface current analysis is also given to understand the operating mechanism of CP wave.

1. Introduction

In recent years, Internet of Things (IoT) gains a rapid growth as being highly valued by commerce, especially in wireless body area network (WBAN). The antennas applied to WBAN are required to equip comprehensive ability due to the complexity of the working environment. In a microwave communication system, the circularly polarized (CP) antennas have potential superiority (e.g., alleviation of multipath losses, resistance to inclement weather, and insensitivity to the device's direction) compared with the linearly polarized (LP) antennas. Generally, the CP wave could be obtained by producing degenerate modes that are 90° out of phase [1]. More and more CP antennas are applied in wireless communication systems such as WiMAX, WLAN, and GPS. A triple-wideband antenna with desirable axial ratio was presented in [2]. Considering that most working situations are not flat case in WBAN, antennas are required to maintain great capability in duplex communication even if frequently bent. Most antennas are not feasible for on-body applications because of hard materials and back radiation to the human body. Therefore, flexible CP antennas with safety attach more attention.

It is inevitable that bending causes performance problems. In order to balance different performances in typical cases, safe wearable patch antennas with foam substrate were presented in [3, 4]. For conveniences and avoiding excessive bending simultaneously, miniature wearable antennas are more acceptable [5]. Thanks to the electroconductivity, ductility, and easy to integrate in garment, conductive textile performs well in WBAN and makes smart garment possible [6–9]. Polydimethylsiloxane (PDMS) is a good candidate for flexible antennas' substrate [10–12]. Due to its fabricating process, the accuracy is inferior to automated printing technologies. Three-dimensional (3D) printing technologies are popular recently, which could produce more solutions in novel antennas to some extent, such as stereolithography, selective laser sintering, and fused deposition modeling (FDM) [13]. FDM offers more possibility to combine multiple materials because of using layer-by-layer deposition to manufacture.

In this work, we propose an embedded antenna with suppressed backward radiation and suitable for wearable devices in the ISM band (at 2.45 GHz) and WiMAX band (at 2.5 GHz). The CP wave is achieved, and the 3 dB axial ratio bandwidth is around 70 MHz (i.e., covers the ISM band (at

2.45 GHz)). In addition, the antenna is fabricated by the FDM technique, and NinjaFlex and conductive fabric are selected as substrate and conductor, respectively. NinjaFlex is characterized by a flexibility value of 85 A on the materials' flexibility shore scale, insulativity, and chemical resistivity [14]. Conductive fabric is further encapsulated by the NinjaFlex layers. All the aforementioned techniques obtain less multipath losses, inclement weather resistance, conformality, flexibility, easy realization, robustness, water resistance, safety, and chemical stability. As far as we know, this is the first-ever CP antenna based on the NinjaFlex-embedded conductive fabric.

2. Antenna Design and Fabrication

2.1. Design. The proposed CP antenna is shown in Figure 1. Considering its superiority in low profile, easy conformality, and safety for the body, a modified square patch antenna with a full ground plane was designed. The full ground plane significantly offers isolation between the antenna and the human body to avoid affecting each other. Furthermore, the proposed antenna was fed by a 50 ohm microstrip line owing to its advantages of low cost, easy to integrate into RF circuit, and more comfortable than a coaxial probe feeding. To obtain CP property, two chamfers and one slot were designed. As seen in Figure 1, the modified square patch was placed on the NinjaFlex substrate. The substrate's thickness is h_s, its dielectric permittivity is 3.0, and its loss tangent is 0.06 [15]. The NinjaFlex has been used in flexible antennas and RFID [16–18].

In order to improve antenna concealment and protect the conductor from water and chemical damage, the entire antenna was encapsulated by NinjaFlex cover (i.e., two NinjaFlex layers were used to cover the top and the bottom). The top encapsulation layer helps in reducing the square patch size slightly, but the bottom layer does not almost have effect on the performance of the antenna. This encapsulation could avoid damaging from washing and excessive bending. To realize the conductor parts, copper foil was used in flexible antennas frequently [19, 20]. The copper foil may crack when excessive bending occurs frequently. Conductive fabric is a good candidate owing to considerable ductility and conductivity. Thus, a fabric coated with silver was employed as a conductor.

An optimization program is further pursued in ANSYS HFSS v15. The optimized dimensions are given in the caption of Figure 1. The designed antenna resonates at around 2.5 GHz and its bandwidth covers the ISM band (at 2.45 GHz) and WiMAX band (at 2.5 GHz).

2.2. Fabrication. The proposed antenna prototype was made by a JGAURORA 3D printer, which is in the FDM technology with a 1.75 mm nozzle for printing. The filament was installed on the right side of the printer and it extended to the nozzle through a filament tube, as shown in Figure 2. Because of its transparent character, the filament with watercolor was selected. In addition, the printing speed was set to 35 mm/s with a nozzle printing temperature of 235°C and

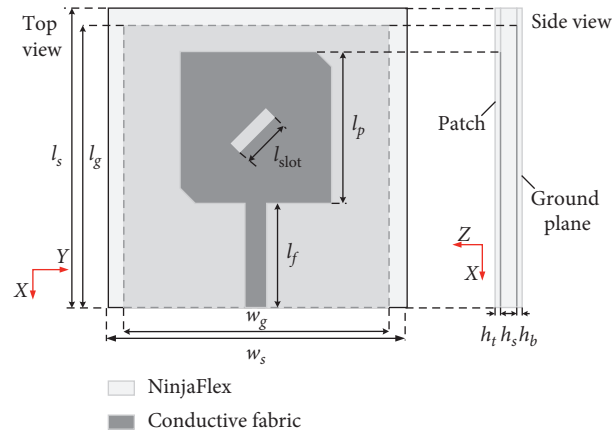

Figure 1: Dimension details of the proposed antenna ($l_s = w_s = 60$, $l_g = 56$, $w_g = 52$, $l_f = 18$, $l_p = 32.3$, $l_{slot} = 12$, $h_s = 1.8$, and $h_t = h_b = 0.6$). All dimensions are in millimeters.

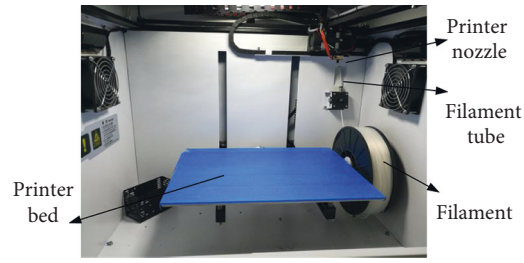

Figure 2: JGAURORA 3D printer.

a bed temperature of 60°C. The rectilinear infill pattern was adopted for all layers, independently from the infill percentage [15]. In the 3D printing process, the stack of layers could be selected to a large extent; consequently, the substrate was printed by 18 solid layers and the thickness of every printing layer is 0.1 mm with an infill of 100%, as shown in Figure 3. This design of stack and infill is significant for the wearable antenna to ensure a solid structure in mechanical properties, as well as to avoid that the air in the cellular structure (i.e., there is more air in the substrate when the infill density is lower) affects the performance of the antenna when the antenna is bent. Due to the fact that the high precision setting extends printing time, the printing process takes about 2 hours and 14 grams of filament.

The electromagnetic characters of the fabricated substrate should be reconfirmed, because the used printer and the layer height were little different from those in [15]. The ring-resonator technique was adopted to determine the effective permittivity of the substrate from the analysis of the resonance frequencies of the ring and the loss tangent from the evaluation of the quality factor of the ring resonances [21]. The ring resonator was designed to achieve the first resonance at 2.4 GHz by assuming a dielectric permittivity of 3.0, and for a substrate thickness of 1.8 mm. The electromagnetic characters were measured from the ring resonator; as a result, the dielectric permittivity is 3.0 and the loss tangent is 0.06 in this fabrication of NinjaFlex.

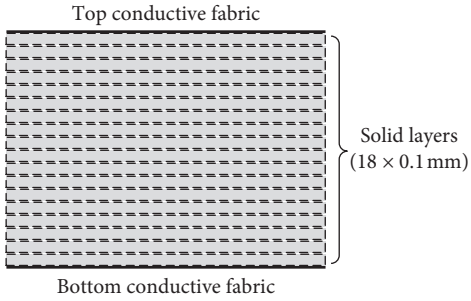

Figure 3: 3D printed NinjaFlex substrate: stack of printed layers.

This fabric's key advantages are the characters conforming to wearable devices. The thickness is 0.2 mm and its sheet resistance is less than 0.06 Ω/sq. The conductive fabric was adhered to both sides of the substrate according to the designed structure. In order to avoid the conductive fabric being scorched by the high temperature of a soldering process, the silver-epoxy adhesive was applied to connect conductive fabric and a SMA connector. Then, the two NinjaFlex layers were adhered to the antenna to achieve the CP antenna based on the NinjaFlex-embedded conductive fabric. The fabricated prototype is shown in Figure 4.

3. Antenna Performance

3.1. Surface Current Distributions. CP radiation can be performed by two orthogonal resonant modes with a 90° phase difference and equal amplitude. In order to understand the CP property, simulated distributions of the surface current of the proposed CP antenna are illustrated in Figure 5, operating at 2.45 GHz with 0°, 90°, 180°, and 270°. As observed, the direction of the surface current is marked. The primary current tendency is in the $+x$-direction when the phase is at 0°. And the main current changes to the $+y$-direction after a 90° phase. Further, the dominant current is in the $-x$-direction while the phase reaching 180°. Finally, the main distributions of the current turns to the $-y$-direction for 270°. Consequently, the right-hand circular polarization (RHCP) wave is realized in the $+z$-direction as the directions of the surface current rotating anticlockwise.

3.2. Return Loss. The return loss (S_{11}) measurements were conducted on the fabricated textile antenna by an Agilent E5070B vector network analyzer in free space and on the human body. As can be seen in Figure 6(a), the total −10 dB bandwidth of return loss is around 275 MHz in the flat case, and the measured result is different from the simulated result slightly. This could be explained with the inaccuracy of fabrication tolerances and SMA connection. In order to validate the impact on performances when the proposed antenna operates in bent situations, the CP antenna was measured while bent in two directions, x-axis and y-axis, with the bending radius of 25 mm and 50 mm, respectively. The bending radius of 25 mm represents the worst situation, corresponding to the typical size of a human wrist. The bending radius of 50 mm corresponds to the representative size of a body arm. However, the bending radius will be greater while being embedded into a garment. A foam was used in measurement as a support, as shown in Figure 7. The results in all situations are shown in Figure 6. As observed, compared with the flat case, the measured resonance frequency shifts up by 3.1% and 2.9% for bending 50 mm along the x-axis and y-axis, respectively. The antenna still maintains more than 300 MHz bandwidth in the 25 mm bending radius, even though the antenna resonance frequency shifts up by 1.2% and 1.6% along the x-axis and y-axis, respectively. Although all the measured results are different from the simulated results, the bandwidth always covers the ISM band (at 2.45 GHz) and WiMAX band (at 2.5 GHz). More importantly, it still returns to intact state after bending.

The on-body testing was also implemented for all situations, and the fabricated textile antenna was placed on a man's wrist and arm to measure in two directions. These two positions are the real situations when the antennas are used on the human body, which correspond to 25 mm and 50 mm in bending radius. It could be regarded as the flat case that the antennas are placed on the human back. As shown in Figure 8, the solid curves and the dashed curves represent the measurement in free space and on the human body, respectively. Resonant frequencies of all the situations on the human body shift slightly compared with those in free space, but the textile antenna still maintains the original trend in the frequency range.

3.3. Far-Field Characteristics. Far-field characteristics were measured using a chamber. As observed in Figure 9, all the measured results shift slightly compared with the corresponding simulated results, but always maintain about 70 MHz 3 dB bandwidth of axial ratio. The CP bandwidth covers the ISM band (at 2.45 GHz) in the flat case. The CP antenna should avoid being bent to 25 mm of the radius as its AR bandwidth shifts away in this case. However, we could obtain almost 160° range of θ at xz-plane when working in flat and bending in the x-direction with 50 mm cases in 2.45 GHz as shown in Figure 10. The radiation patterns in all cases were measured and compared with the results of simulations in Figure 11. As expected, all the measured results change slightly compared with those in simulations, and desirable low backward radiation is achieved, which means little impact on the human body. The radiation pattern is headed toward the positive z-direction. Furthermore, simulated and measured efficiency, peak gain, and directivity in all situations are listed in Table 1. "s/m" in Table 1 means "simulated/measured." In flat situation, the antenna has 25.8% of efficiency and 0.96 dBi of peak gain.

3.4. Specific Absorption Rate. Specific absorption rate (SAR) is also a significant characteristic while considering the safety of the wearable devices for the human body. The lower the SAR, the less is the electromagnetic impact on the body.

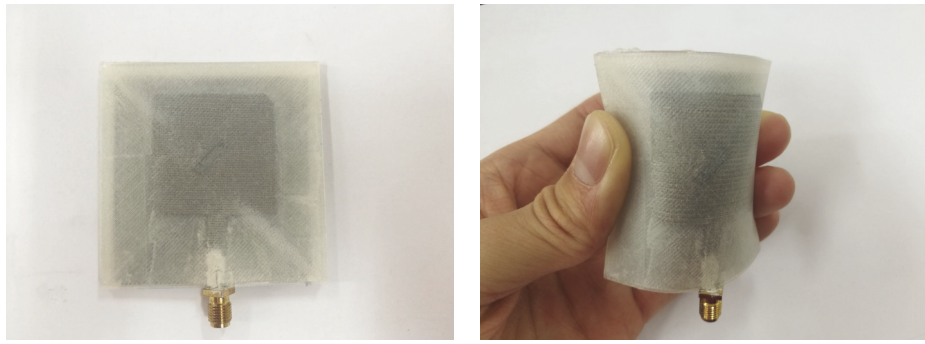

(a) (b)

Figure 4: Photographs of the fabricated CP antenna. (a) Top view. (b) Bent view (bending along the y-axis).

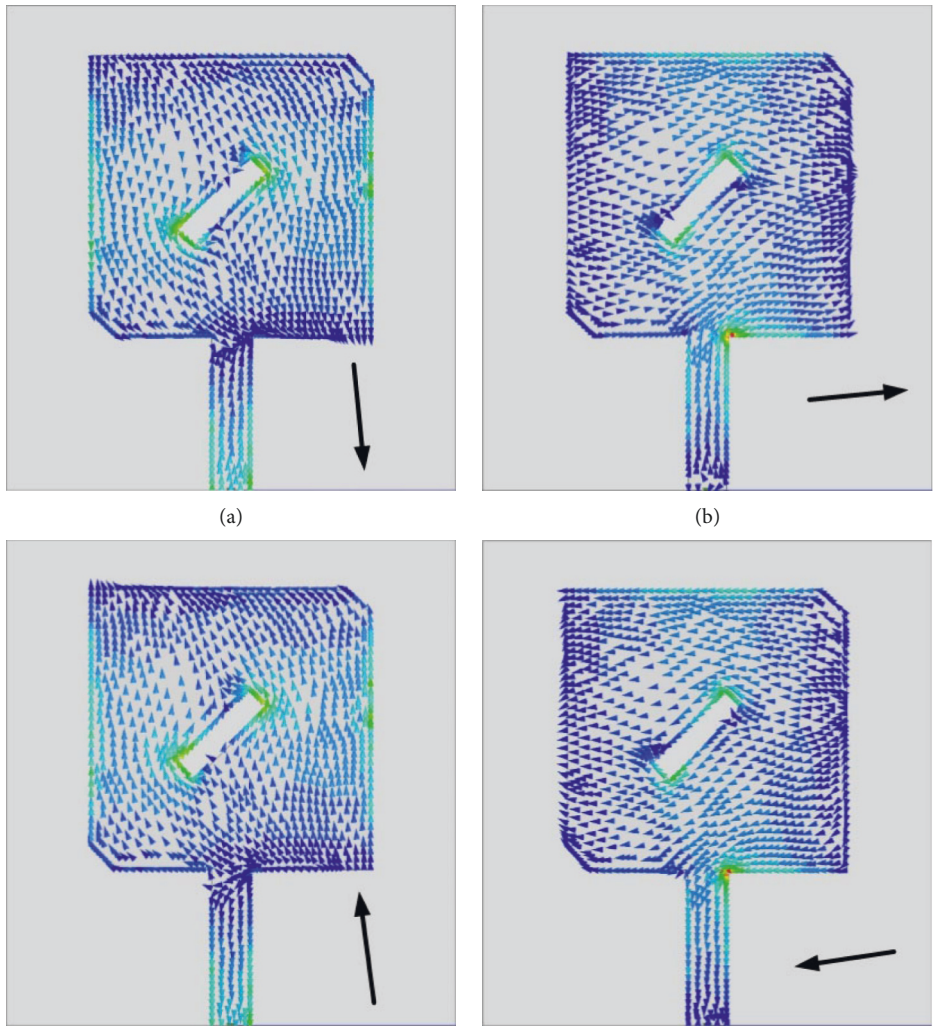

(a) (b)

(c) (d)

Figure 5: Distributions of the surface current on the proposed antenna at 2.45 GHz with different phase angles: (a) 0°, (b) 90°, (c) 180°, and (d) 270°.

The SAR value is calculated with 1 watt input power averaging in 1-gram tissue in ANSYS HFSS v15. Furthermore, all aspects of this calculation (e.g., the properties of the flat phantom and requirements of tissue) conform to IEEE 1528 standard [22]. The peak SAR result of the proposed CP antenna (0.6 W/kg at 2.45 GHz) is much lower than the FCC

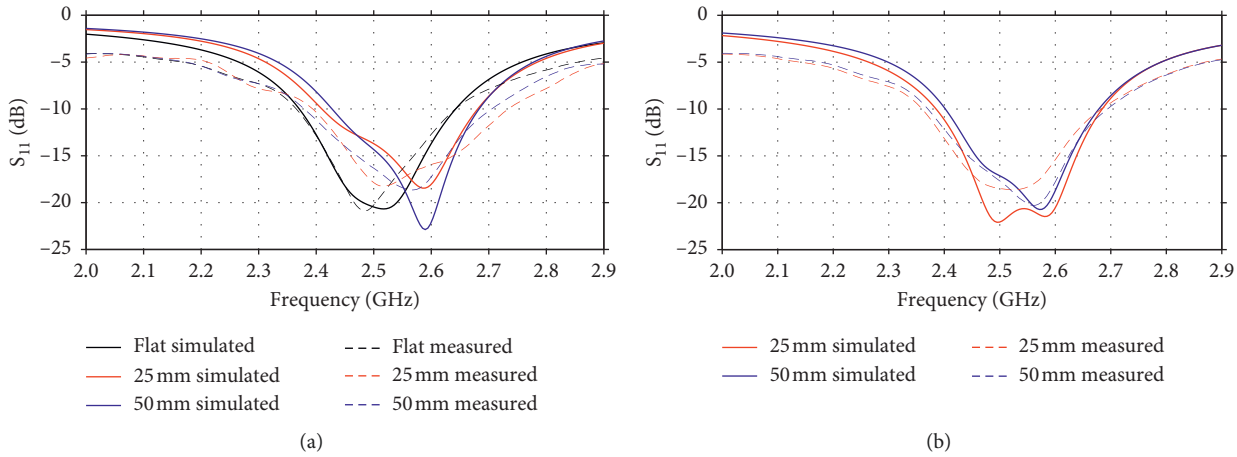

Figure 6: Simulated and measured S_{11} curves with different radii. (a) Bending along the x-axis. (b) Bending along the y-axis.

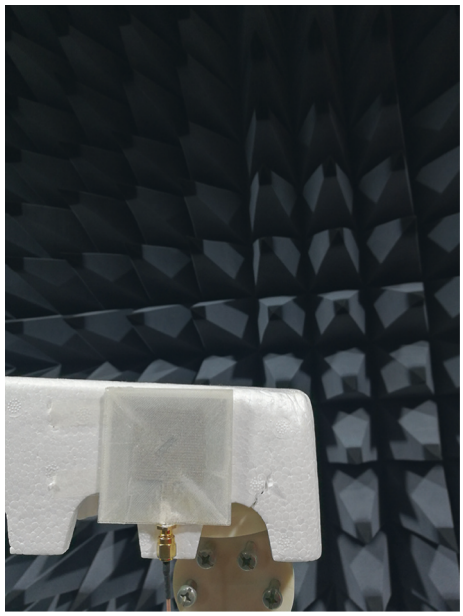

Figure 7: The measurement in the chamber.

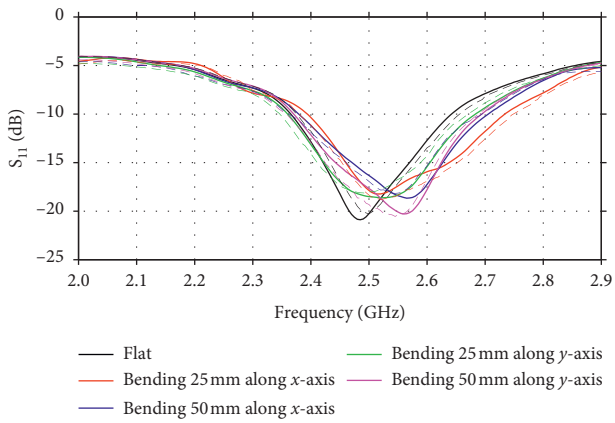

Figure 8: Measured S_{11} in free space (solid curves) and on the human body (dashed curves).

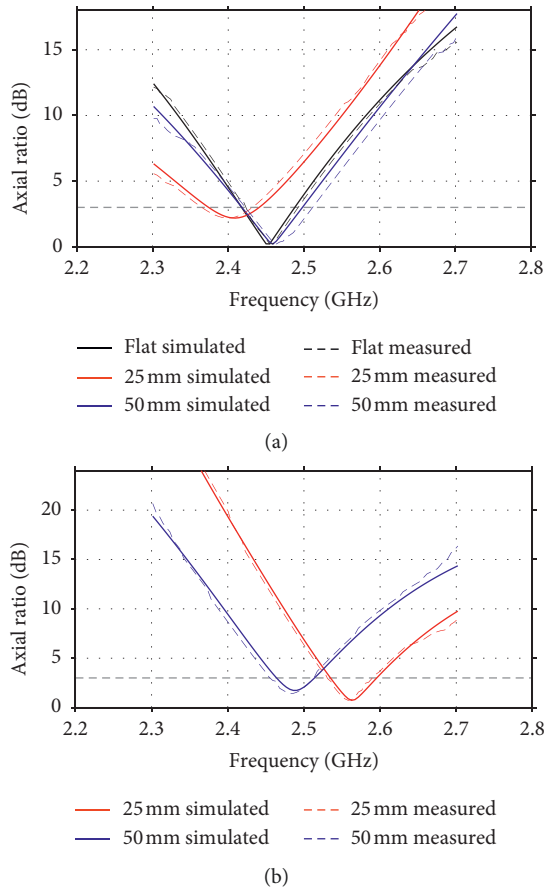

Figure 9: Simulated and measured AR: (a) x-axis bending and (b) y-axis bending.

limitation (1.60 W/kg) owing to the full ground of the proposed antenna. This result further testifies that the proposed flexible CP antenna is feasible for on-body devices.

3.5. Effect of Washing. The proposed wearable antenna was further verified by a washability examination. It was finished

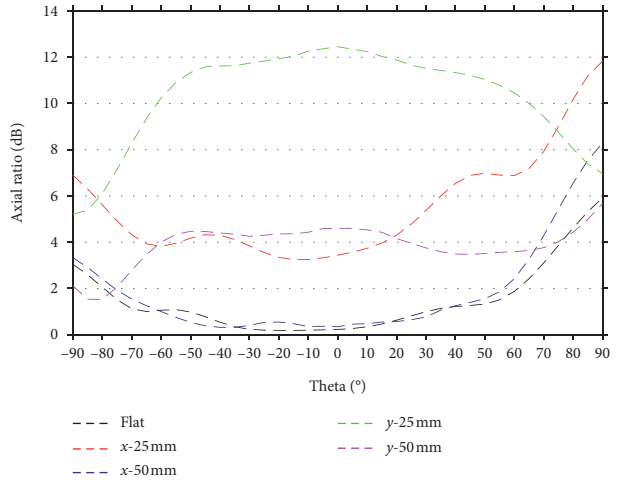

Figure 10: Measured AR in flat and bent x- and y-directions at 2.45 GHz at $\varphi = 0^{\circ}$.

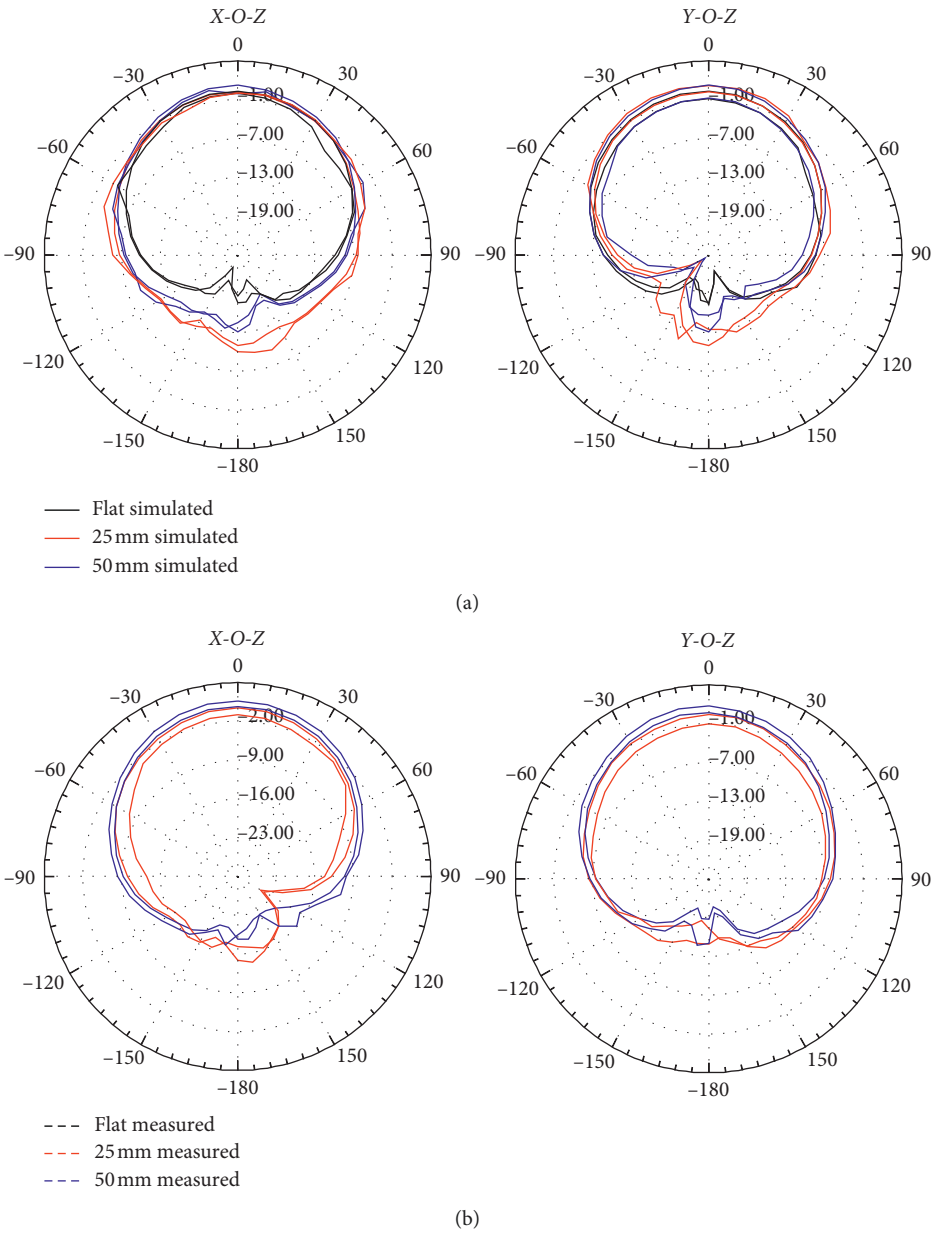

Figure 11: Simulated and measured radiation patterns in different bending directions: (a) x and (b) y. All the values are in dB.

Table 1: Simulated and measured efficiency, peak gain, and directivity in all situations.

	Efficiency: s/m	Peak gain: s/m (dBi)	Directivity: s/m (dBi)
Flat	25.9%/25.8%	0.97/0.96	6.83/6.84
Bending 25 mm along x-axis	27.6%/27.5%	0.63/0.60	6.22/6.21
Bending 50 mm along x-axis	30.9%/30.7%	1.82/1.80	6.93/6.93
Bending 25 mm along y-axis	29.2%/29.1%	1.13/1.11	6.48/6.47
Bending 50 mm along y-axis	29.9%/29.8%	1.43/1.42	6.64/6.68

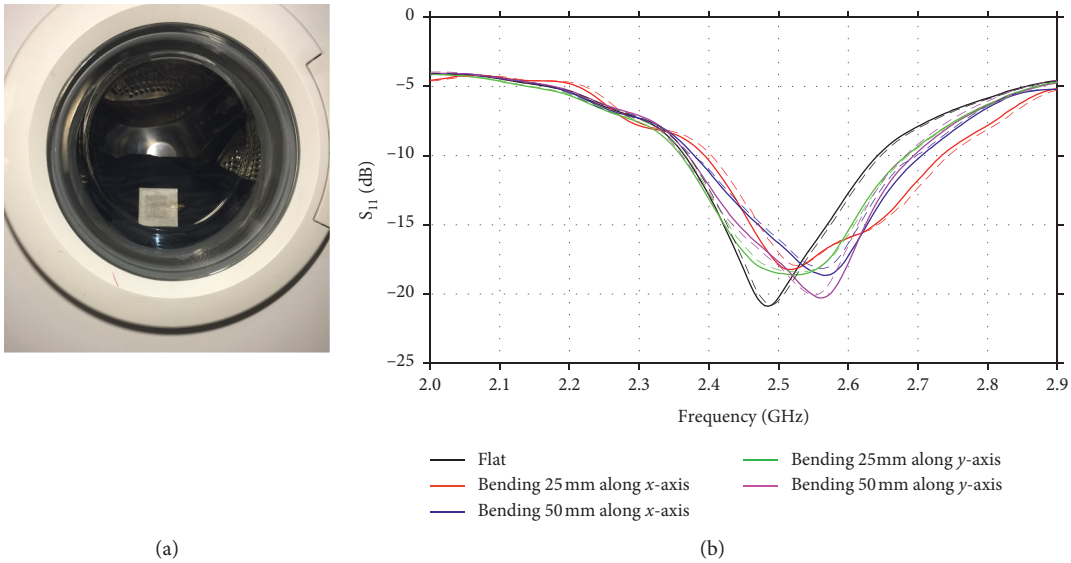

(a) (b)

Figure 12: Washing test. (a) Antenna in the washing machine. (b) Measured S_{11} before (solid curves) and after (dashed curves) washing.

Table 2: Comparison of flexible antennas reported in the literature.

Ref.	Substrate	Conductor	Peak gain (dBi)	BW (%)	Max Δf (%)	Efficiency (%)	ARBW (MHz)	Washability
[3]	EVA	Copper gauze	4.36	5.2	1.2	51	—	No
[15]	NinjaFlex	Copper	−3.8	5.5	3	18	—	No
[19]	SU-8/PDMS	Copper	2.17	3	5.8	—	—	No
This	NinjaFlex	Silver fabric	1.8	11	3.1	30.7	70	Yes

through washing the antenna in a household washing machine with detergent and water at 35°C. The wearable antenna was washed with a quick mode for 30 minutes, as shown in Figure 12(a). The SMA connector was protected by a plastic cap and a tape to avoid the amount of water flowing into it. The measured results in return loss, before washing (solid curves with different colors) and after washing (dashed curves with different colors), are compared in Figure 12(b). As expected, the fabricated antenna still maintains consistent performances in all situations even if bending along two directions. The NinjaFlex layers offer protection to resist water during washing. The little changes in the band may be caused by the part of connection that was bent slightly during the turbulence in the washing machine.

4. Comparison of Antenna Performance

Finally, a comparison of flexible antennas reported in references and this paper is given in Table 2. These antennas used different manufacturing technologies. From Table 2, the design presented in this paper demonstrates a lower frequency shift and the best bandwidth in comparison with those in prior publications. The proposed CP antenna has good performances in washability and axial ratio bandwidth, compared to those in the prior publications, and the CP antenna also has good ductility as the conductor is ductile.

5. Conclusions

In this paper, a wearable NinjaFlex-embedded conductive fabric CP antenna with a full ground plane is proposed. The antenna prototype has been fabricated successfully by the FDM printing technology. It is flexible with shape stability. To realize the CP property, two chamfers and one slot are employed and the antenna holds around 70 MHz 3 dB AR bandwidth. By encapsulating the antenna into NinjaFlex layers, the flexible antenna is waterproof. In terms of radiation characters, there is a good agreement between simulated and measured results. The presented antenna holds acceptable S_{11} bandwidth (11%) and 160° range of θ at

xz-plane. Furthermore, the SAR is very low, which means safety for the human body. The proposed antenna will be an attractive candidate for WLAN, WiMAX, and WiFi applications on the human body owing to its simple configuration, low profile, CP radiation, wearability, washability, and safety.

Data Availability

The experimental data used to support the findings of this study are available from the corresponding author upon request.

Conflicts of Interest

The authors declare that they have no conflicts of interest.

Acknowledgments

This work was supported by the National Natural Science Foundation of China (Grant no. 61372011) and the Program for Innovative Research Team in University of Tianjin (Grant no. TD13-5040).

References

[1] K. Ding, Y.-X. Guo, and C. Gao, "CPW-fed wideband circularly polarized printed monopole antenna with open loop and asymmetric ground plane," *IEEE Antennas and Wireless Propagation Letters*, vol. 16, pp. 833–836, 2017.

[2] R. Xu, J.-Y. Li, Y.-X. Qi, G.-W. Yang, and J.-J. Yang, "A design of triple-wideband triple-sense circularly polarized square slot antenna," *IEEE Antennas and Wireless Propagation Letters*, vol. 16, pp. 1763–1766, 2017.

[3] H. Wang, Z. Zhang, Y. Li, and Z. Feng, "A dual-resonant shorted patch antenna for wearable application in 430 MHz band," *IEEE Transactions on Antennas and Propagation*, vol. 61, no. 12, pp. 6195–6200, 2013.

[4] C. Hertleer, H. Rogier, L. Vallozzi, and L. Van Langenhove, "A textile antenna for off-body communication integrated into protective clothing for firefighters," *IEEE Transactions on Antennas and Propagation*, vol. 57, no. 4, pp. 919–925, 2009.

[5] M. Wagih, Y. Wei, and S. Beeby, "Flexible 2.4 GHz node for body area networks with a compact high-gain planar antenna," *IEEE Antennas and Wireless Propagation Letters*, vol. 18, no. 1, pp. 49–53, 2019.

[6] C. Hertleer, A. Tronquo, H. Rogier, L. Vallozzi, and L. Van Langenhove, "Aperture-coupled patch antenna for integration into wearable textile systems," *IEEE Antennas and Wireless Propagation Letters*, vol. 6, pp. 392–395, 2007.

[7] M. Klemm and G. Troester, "Textile UWB antennas for wireless body area networks," *IEEE Transactions on Antennas and Propagation*, vol. 54, no. 11, pp. 3192–3197, 2006.

[8] Q. Bai and R. Langley, "Crumpling of PIFA textile antenna," *IEEE Transactions on Antennas and Propagation*, vol. 60, no. 1, pp. 63–70, 2012.

[9] E. K. Kaivanto, M. Berg, E. Salonen, and P. de Maagt, "Wearable circularly polarized antenna for personal satellite communication and navigation," *IEEE Transactions on Antennas and Propagation*, vol. 59, no. 12, pp. 4490–4496, 2011.

[10] S. M. Abbas, S. C. Desai, and K. P. Esselle, "Design and characterization of a flexible wideband antenna using polydimethylsiloxane composite substrate," *International Journal of Antennas and Propagation*, vol. 2018, Article ID 4095765, 6 pages, 2018.

[11] H. Mirza, T. Md Hossain, P. J. Soh et al., "Deployable linear-to-circular polarizer using PDMS based on unloaded and loaded circular FSS arrays for pico-satellites," *IEEE Access*, vol. 7, pp. 2034–2041, 2019.

[12] R. B. V. B. Simorangkir, Y. Yang, R. M. Hashmi et al., "Polydimethylsiloxane-embedded conductive fabric: characterization and application for realization of robust passive and active flexible wearable antennas," *IEEE Access*, vol. 6, pp. 48102–48112, 2018.

[13] A. K. Kamrani and E. A. Nasr, "Rapid prototyping," in *Engineering Design and Rapid Prototyping*, pp. 339–354, Springer, Boston, MA, USA, 2009.

[14] https://ninjatek.com/ninjaflex/, 2019.

[15] S. Moscato, R. Bahr, T. Le et al., "Infill-dependent 3-D-printed material based on NinjaFlex filament for antenna applications," *IEEE Antennas and Wireless Propagation Letters*, vol. 15, pp. 1506–1509, 2016.

[16] M. Rizwan, M. W. A. Khan, H. He, J. Virkki, L. Sydänheimo, and L. Ukkonen, "Flexible and stretchable 3D printed passive UHF RFID tag," *Electronics Letters*, vol. 53, no. 15, pp. 1054–1056, 2017.

[17] M. Rizwan, M. W. A. Khan, L. Sydanheimo, J. Virkki, and L. Ukkonen, "Flexible and stretchable brush-painted wearable antenna on a three-dimensional (3-D) printed substrate," *IEEE Antennas and Wireless Propagation Letters*, vol. 16, pp. 3108–3112, 2017.

[18] M. Cosker, L. Lizzi, F. Ferrero, R. Staraj, and J.-M. Ribero, "Realization of 3-D flexible antennas using liquid metal and additive printing technologies," *IEEE Antennas and Wireless Propagation Letters*, vol. 16, pp. 971–974, 2017.

[19] C. P. Lin, C. H. Chang, Y. T. Cheng, and C. F. Jou, "Development of a flexible SU-8/PDMS-based antenna," *IEEE Antennas Wireless Propagation Letters*, vol. 10, pp. 1108–1111, 2011.

[20] H. Li, S. Sun, B. Wang, and F. Wu, "Design of compact single-layer textile MIMO antenna for wearable applications," *IEEE Transactions on Antennas and Propagation*, vol. 66, no. 6, pp. 3136–3141, 2018.

[21] L. Yang, A. Rida, R. Vyas, and M. M. Tentzeris, "RFID tag and RF structures on a paper substrate using inkjet-printing technology," *IEEE Transactions on Microwave Theory and Techniques*, vol. 55, no. 12, pp. 2894–2901, 2007.

[22] IEEE recommended practice for determining the peak spatial-average specific absorption rate (SAR) in the human head from wireless communications devices: measurement techniques amendment 1: CAD file for human head model (SAM phantom), IEEE Std.1528a-2005 (Amendment to IEEE Std. 1528-2003), 2006.